

# Infrared camera measurement of source

R. Drga, D. Janáčová, H. Charvátová

**Abstract**— The paper deals with the infrared radiation source EK-8520, ability to measure using a thermocouple TP334 and temperature by thermal imager for calculating spectral range. It prepares the theoretical and practical bases for testing infrared radiation detectors for security technologies.

**Keywords**— IR radiation, sensor, emissivity, detector, security technology.

## I. INTRODUCTION

THE heat-emitting sources are characterized by broad spectral range, where the spectral maximum is shifting to the rising temperature resource from the far-infrared region to region near the visible spectrum. The aim is to measure the temperature of the source of thermal imager, to determine the spectral maximum amount of energy emitted by source of radiation in our case, the EK-8520 produced by Helioworks, TP334 evaluate the sensitivity of the sensor on this radiation and create the conditions for measurement, especially in the spectral range of about 9 mm.

## II. THEORY

Electromagnetic radiation is a part of our world and a man meets with his influence at every step. The basic senses, which can perceive and recognize this radiation is the ability to see and the skin's ability to perceive blazing heat. Infrared radiation is outside the visible spectrum, see Figure 1.

While the visible spectrum starts at wavelengths 380 nm and ends at 750 nm, the area of infrared radiation wavelength starts at 0.75 and ends at a length of 1000 mm. This is called characteristic radiation. It is caused by internal mechanical movement of molecules.

This work was supported by the Ministry of Education, Youth and Sports of the Czech Republic under the Research Plan No. MSM 7088352102 and by the European Regional Development Fund under the project CEBIA-Tech No. CZ.1.05/2.1.00/03.0089.

R. Drga, Tomas Bata University in Zlín, Faculty of Applied Informatics, Department of Security Engineering, nám. T. G. Masaryka 5555, 760 01 Zlín, Czech Republic (e-mail: mokrejs@ft.utb.cz)

D. Janáčová, Tomas Bata University in Zlín, Faculty of Applied Informatics, Department of Automation and Control Engineering, nám. T. G. Masaryka 5555, 760 01 Zlín, Czech Republic ; phone: +420 576 035 274; fax: +420 576 032 716; e-mail: janacova@fai.utb.cz

H. Charvátová, Tomas Bata University in Zlín, Faculty of Applied Informatics, Department of Automation and Control Engineering, nám. T. G. Masaryka 5555, 760 01 Zlín, Czech Republic (e-mail: charvatova@fai.utb.cz)

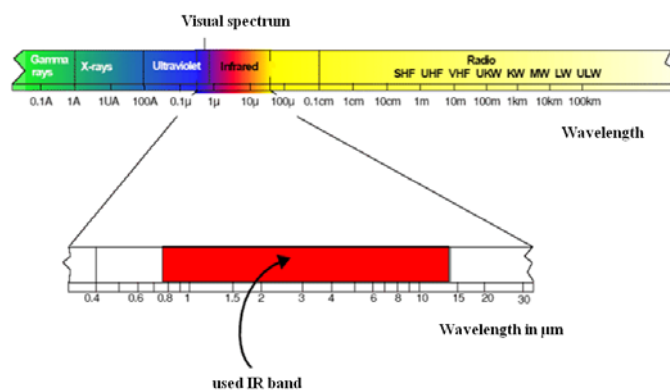


Fig. 1 Electromagnetic spectrum

The intensity of this movement depends on the temperature of the object. Because the movement of molecules is a moving charge is emitted electromagnetic radiation (photon particles). These photons are moving at light speed and behave according to known optical laws. They can be diverted, concentrated lenses or reflected by reflective surfaces. By the customary conventions for infrared spectroscopy and for practical reasons are divided wavelengths of radiation to the area close to (A - NIR - Near infrared) 750-900 nm, medium (B-MIR - Middle infrared) from 1.55 to 1.75 micron and far (C - FIR - Far Infrared), 10.4 to 12.5 micron according to field use.

To measure the amount of incident light are used photodetectors, which can be divided according to function on the detectors with direct conversion of radiation into electrical energy and indirect principles.

## DIRECT ENERGY CONVERSION

Photodetectors with a direct conversion of energy are subdivided according to the principle of two basic groups according to the photoelectric effect.

External photoelectric effect:

Photocells  
Photomultiplier

Internal photoelectric effect:

Photoresistor  
Photodiodes  
Phototransistors,  
MSM photodetectors

## INDIRECT ENERGY TRANSFORMATION

These detectors are based on the conversion of radiant energy into heat. Changes in temperature affect the electrical properties of the detector. Typical representatives of this category are:

thermocouple  
pyroelectric detectors  
bolometer

In the next section I will devote the infrared where detectors are primarily used with indirect conversion of heat. Areas where it is used directly by measuring the infrared radiation can be divided three sections as follows:

Measurements of surface temperatures in the industry  
Measuring temperature properties of objects in security and safety technologies

Measuring of gases – spectroscopy

In security this principles are use used in this detectors:

PIR detectors  
IR camera  
IR illumination for cameras  
IR barriers and gates  
IR scanner for facial recognition  
Noktovizor

In safety or fire alarms systems are used these detectors:

Flame detectors and flame detector matrix  
Linear detector of smoke  
Smoke detectors

## BALANCE OF ENERGY RADIATED

Each matter at a temperature above absolute zero ( $-273^{\circ}\text{C}$ ) emits infrared radiation, whose intensity corresponds to its temperature. The diagram on Fig. 2 shows the characteristics of the radiation at different body temperatures. It shows that objects at high temperatures emits a small quantities of visible radiation. Therefore, we can see these objects at high temperatures (above  $600^{\circ}\text{C}$ ) in colors ranging from red and white. Experienced lead smelter estimate the temperature of iron according to the color quite accurately. Since 1930 is used in steel mills and ironworks visual pyrometers with a disappearing filament. The invisible part of the spectrum however contains up to 100 000 times more energy. On this fact puts infrared technology. The diagram also shows that the maximum radiation inches toward ever shorter wavelengths when the temperature increases measured object and a body that curves at different temperatures overlap.

Radiated energy in the entire wavelength range (area under each curve) increases with the 4th power of temperature

according to the Stefan-Boltzmann law, see equation (1) and it is clear that the emitted signal can be determined by temperature

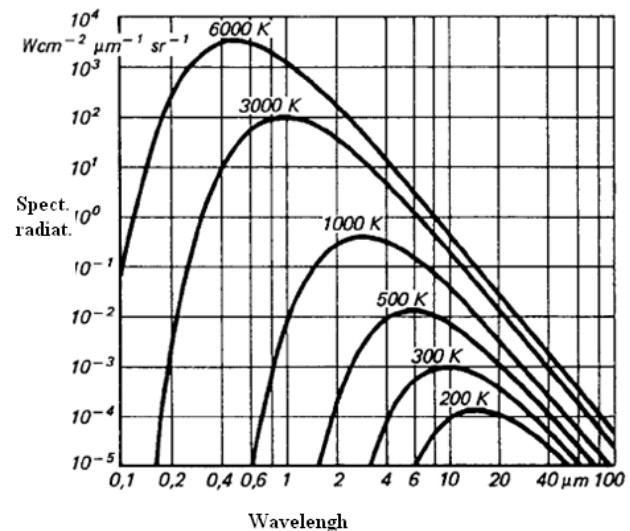


Fig. 2 Radiation diagram of absolute black body on temperature

$$Q_0 = H_0 \cdot S_1 = \delta_0 \cdot T^4 \cdot S_1 \quad (1)$$

where  $Q_0$  is the total energy radiated per unit time per unit area of an absolutely black body  $H_0$  is the total radiation intensity ( $\text{W}/\text{m}^2$ ),  $S_1$  is the area of the black body,  $T$  is absolute temperature of the body and  $\delta_0$  is the Stefan-Boltzmanova constant [K. Kolomazník, 1988].

From Fig. 2nd Radiation characteristics of an absolutely black body, depending on its temperature is evident that the ideal would be to set up an infrared thermometer to the widest possible wavelength range to obtain as much energy (corresponding to the area under the curve), or the measured signal from the body. But there are some cases in which it is not always convenient. For example, the diagram intensity of radiation at 2 micron increases more with increasing temperature than at 10 mm. The greater the difference radiation at a certain temperature difference, the more infrared thermometer works. Using the Wien's displacement law, see equation 2 on the maximum emission shift to shorter wavelengths with increasing temperature, then corresponds to a range of wavelengths measuring pyrometer temperature

$$\lambda_{\max} = \frac{b}{T} \quad (2)$$

where  $\lambda_{\max}$  is the wavelength of maximum radiation,  $T$  is temperature and  $b$  is the body Wien constant, which value is approximately

$$b = 2,898 \text{ mm} \cdot \text{K} \quad (3)$$

Spectral density of radiation the maximum is proportional to the fifth power of temperature

$$W_{\lambda} = const.T^5 \quad (4)$$

At low temperatures below 600 ° C infrared thermometer operating at 2 micron could see almost nothing, because it would be too little radiated power. Another reason for the production of devices with different wavebands is emissivity property of certain materials known as "non-gray bodies" (eg glass, metal and plastic coatings). The diagram on Fig. 2 shows the ideal radiation, which is called "black body" radiation. Many bodies, at the same temperature emit less energy. The relationship between the actual radiated energy and the energy radiated by the same black body temperature is known as the emissivity  $\epsilon$  (epsilon) and can have a maximum value of 1 (in this case body conforms to the ideal black body) and the minimum value of 0. Body with emissivity less than 1 is called gray bodies. Bodies, which emissivity are also dependent on temperature and wavelength are called non-gray bodies (non-gray Bodies). The total radiation balance of the real body is shown in Figure 3. The total amount of radiated energy is composed of radiation emitted by the body's own  $E$ , there is increasing  $R$  radiation reflected from the heat source  $I$  even before the measured object and the radiation passing through the measured object  $T$  from the heat source located behind the measured object. According to the equation

$$E + R + T = I \quad (5)$$

the total sum equal to 1 [D. Janáčková, 2010]

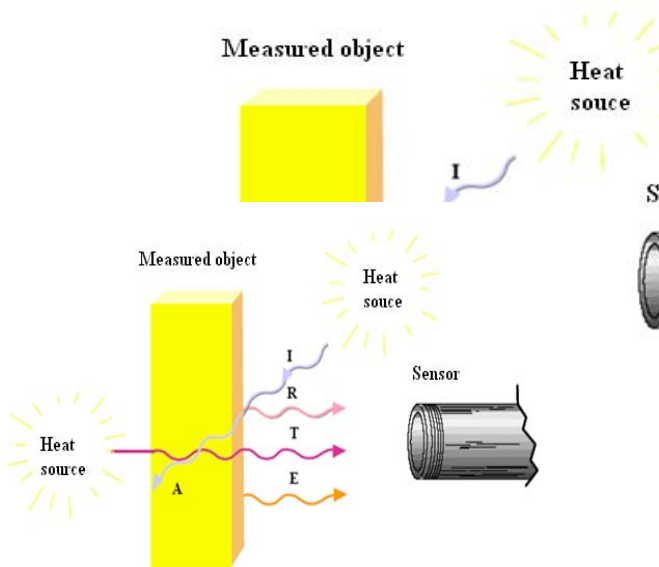


Fig. 3 All balance of radiations of real body

The real body as opposed to absolutely black body is not able to radiate all the energy and this is therefore given by

$$Q_S = \epsilon. Q_0 = \epsilon. H_0. S_1 = \epsilon. \delta_0. T_4. S_1 \quad (7)$$

where  $\epsilon$  is the emissivity coefficient of the object

Object emissivity is equal to the ratio of radiation intensities real surface and the surface of an absolutely black body. Real bodies are mostly non-gray bodies and they have characteristics dependent on the wavelength, see Fig. 4. Many non-metallic materials such as wood, plastic, rubber, organic materials, stone or concrete with a surface that reflects very little, and therefore have a high emissivity between 0.8 and 0.95. On the contrary, metals – particularly those with polished or glossy finish – have an emissivity around 0.1. E.g. mirror has emissivity, which is close zero. Infrared thermometers offer a compensating adjustment variables emissivity factor. It practically solves the fact, that the measured surface stick sticker, which has a surface, which emissivity approaching value of absolute black body, we measure this area and then point the thermometer besides this area, measure this area and set coefficient of emissivity to match the temperature of the originally measured temperature.

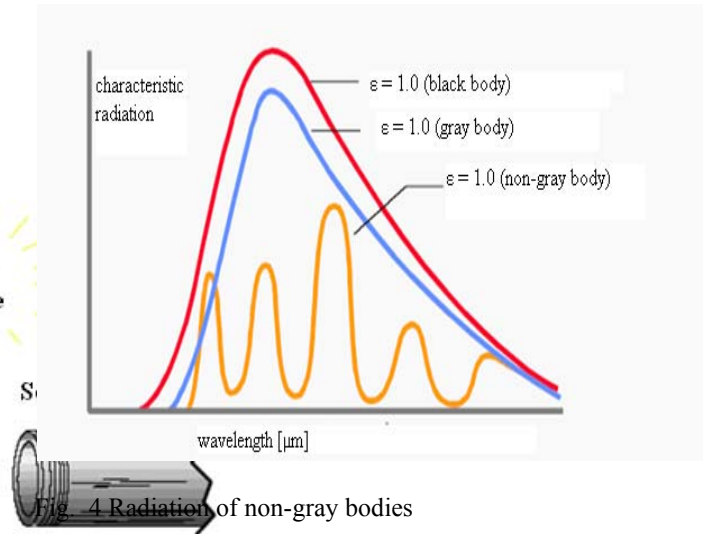


Fig. 4 Radiation of non-gray bodies

The emissivity of metals is directly dependent on the wavelength and temperature of the material and therefore, if we filter the input device to a particular wavelength, we can commit errors of measurement, which explains the shift Wien law of spectrum (2) see Figure 5

Now we will talk about PIR – passive infrared detectors - figure 2. The term 'passive' in this instance means the PIR does not emit any energy of any type but merely sits 'passive' accepting infrared energy through the 'window' in its housing.

The heart of the sensor is a solid state chip made from a pyroelectric material.

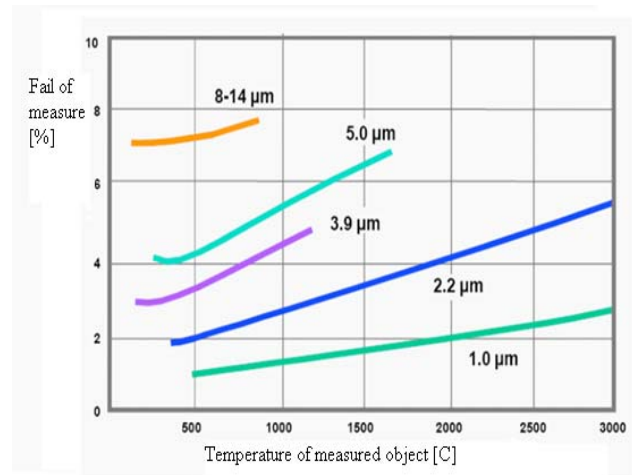


Fig. 5 Fails of temperature measurement caused

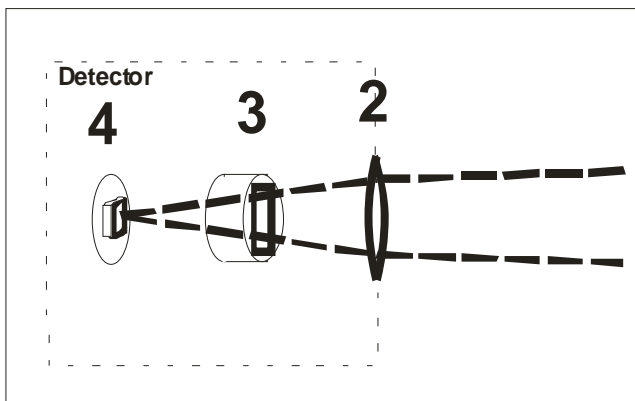


Fig. 6 Principle of detector with Fresnell lens

On the figure 6 pyroelectric detector (4) in this configuration intended to monitor radiation coming through optical filter (3) with a wavelength near 10 microns and through Fresnel lens (2). Real way of energy is shown on figure 7.

The energy from absolutely black body using Stefan-Boltzmann law is (1)

where  $H_0$  is all intensity of radiation ( $W/m^2$ ),  $S_l$  is square of body,  $T$  is absolute temperature of body and  $\delta_0$  is Stefan-Boltzmann constant (3)

In real situation, when the body is grey, then the energy from object 1 to Fresnel lens is

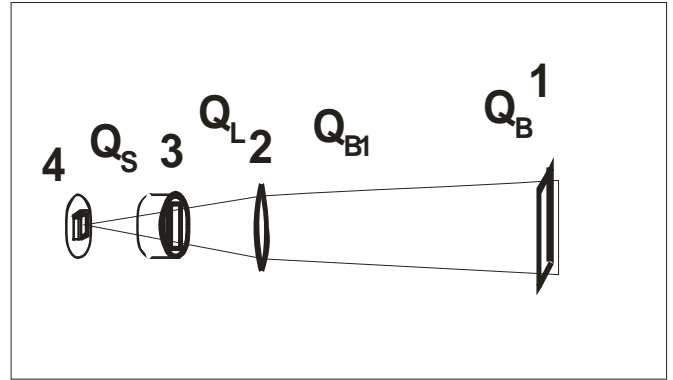


Fig. 7 All way of energy with Fresnel lens

$$Q_B = \delta_0 \cdot S_l \cdot (\epsilon_l \cdot T_l^4) \tag{8}$$

Where  $\epsilon_l$  is coefficient of emissivity of body 1 (-)  
Energy coming to Fresnel lens is

$$Q_{B1} = \delta_0 \cdot S_l \cdot (\varphi_l \cdot \epsilon_l \cdot T_l^4) \tag{9}$$

Where  $\varphi_l$  is angle coefficient (-)  
Energy coming through Fresnel lens is

$$Q_L = \delta_0 \cdot S_l \cdot (\tau_l \cdot \varphi_l \cdot \epsilon_l \cdot T_l^4) \tag{10}$$

Where  $\tau_l$  is coefficient of penetration of plastic Fresnel lens (2) (-)  
Then the energy coming through filter to pyroelectric chip is

$$Q_S = \delta_0 \cdot S_l \cdot (\tau_2 \cdot \tau_l \cdot \varphi_l \cdot \epsilon_l \cdot T_l^4) \tag{11}$$

Where  $\tau_2$  is coefficient of penetration of filter (3) (-)  
Finally

$$Q_M = Q_S(\alpha + \rho + \tau_s + \delta_0 \cdot S_s \cdot \epsilon_s \cdot T_s^4) \tag{12}$$

where  $Q_M$  is methodical energy,  $\alpha$  is coefficient of polarization of pyroelement,  $\rho$  is coefficient of reflection  $\tau_s$  is coefficient of penetration and  $\delta_0 \cdot S_s \cdot \epsilon_s \cdot T_s^4$  is energy back emitted

Voltage in output of pyroelement is

$$U_{out} = k_{pe} \cdot Q_M \tag{13}$$

and  $k_{pe}$  is constant of sensitivity of pyroelement (V/W)

Similar situation we can see, when we use mirror, see figure 3.

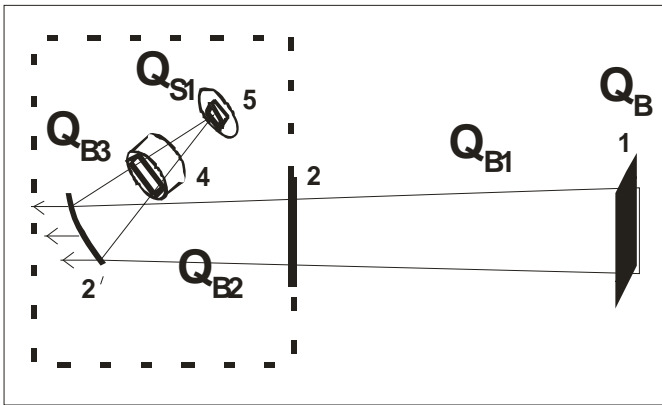


Fig. 8 All way of energy from source to pyroelectric element using mirror

Grey body (1) emits energy  $Q_B$  to plastic shield 2

$$Q_{B1} = \delta_0 \cdot S_1 \cdot (\varphi_1 \cdot \varepsilon_1 \cdot T_1^4) \quad (14)$$

Where  $\varepsilon_1$  is coefficient of emissivity of body (1) (-) and  $\varphi_1$  is angle coefficient (-)

Energy coming through plastic shield is

$$Q_{B2} = \delta_0 \cdot S_1 \cdot (\tau_3 \varphi_1 \cdot \varepsilon_1 \cdot T_1^4) \quad (15)$$

Where  $\tau_3$  is coefficient of penetration of plastic shield 2 (-)  
Then the energy coming to mirror (2)

$$Q_{B3} = \delta_0 \cdot S_1 \cdot (\rho_1 \tau_3 \varphi_1 \cdot \varepsilon_1 \cdot T_1^4) \quad (16)$$

Where  $\rho_1$  is coefficient of reflection (-) of mirror. This is most important property of the system, because false emission is absorbed and measured emission is reflected.

Then the energy coming through filter to pyroelectric chip is

$$Q_{S1} = \delta_0 \cdot S_1 \cdot (\rho_1 \tau_3 \tau_2 \tau_1 \varphi_1 \cdot \varepsilon_1 \cdot T_1^4) \quad (17)$$

Where  $\tau_2$  is coefficient of penetration of filter 3 (-)

$$Q_{M1} = Q_{S1}(\alpha + \rho + \tau_s + \delta_0 \cdot S_s \cdot \varepsilon_s \cdot T_s^4) \quad (18)$$

where  $Q_{M1}$  is methodical energy,  $\alpha$  is coefficient of polarization of pyroelement,  $\rho$  is coefficient of reflection  $\tau_s$  is coefficient of penetration and  $\delta_0 \cdot S_s \cdot \varepsilon_s \cdot T_s^4$  is energy back emitted

Voltage in output of pyroelement is

$$U_{out} = k_{pe} \cdot Q_M \quad (19)$$

and  $k_{pe}$  is constant of sensitivity of pyroelement ( V/W).

In Figure 9 we can see all radiation sources, which are able to detect motion detector (2) and its pyroelement (1). It is especially useful radiation (3), which comes from the object (4), whose movement and existence we want to detect. Another source of variable light (8) is the sun (7) and ambient influences. The last source of radiation (6) is a stable source of background radiation (5) and when it has slow changes of temperature, it can be useful for detecting intruders.

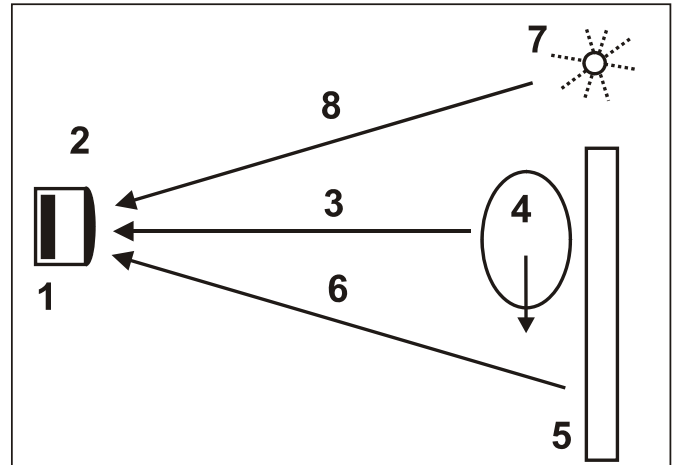


Fig. 9 All source of radiation of PIR detector

The main problem for exact measurement of PIR detectors is a source of infrared radiation, whose properties would be precisely defined and adjustable. The heat-emitting sources are characterized by broad spectral range, where the spectral maximum is shifting to the rising temperature resource from the far-infrared region to region near the visible spectrum. The aim is to measure the temperature of the source of thermal imager, to determine the spectral maximum amount of energy emitted by source of radiation in our case, the EK-8520 produced by Helioworks see. Figure 10 The actual structure consists of a metal casing 2, in which the holders fixed helix 1, followed by a gold mirror placed third Radiation after reflection is rectified according to Figure 4 For some types of window is covered with a transparent material that has characteristics of the optical filter.

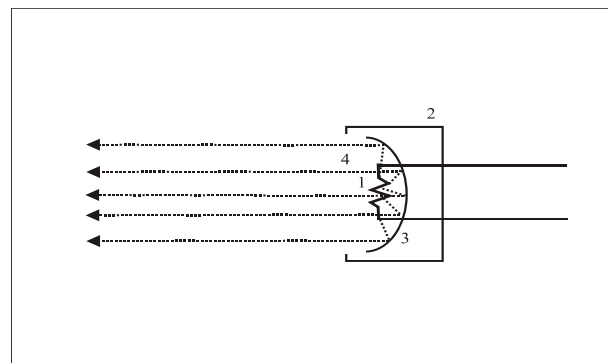


Fig. 10 Heat IR source EK-8520

We have to realize measure workplaces with instruments for measuring of radiation and optical properties of sources and sensors. The workplace is symbolically illustrated in Figure 11 and consists of a regulated DC power supply 2 with the possibility to limit the maximum current to avoid damage of the IR radiation source. In the brass holder 3 is placed source IR 8520 EC so that the emitted infrared radiation reflected from the inner gold-plated dish so that is not overshadowed by brass holder and is all directed to the brass plated tube 4 in the direction of the IR camera. The metal tube is 10 cm long, the camera is placed at 15 cm distance from the source of the EC 8520.

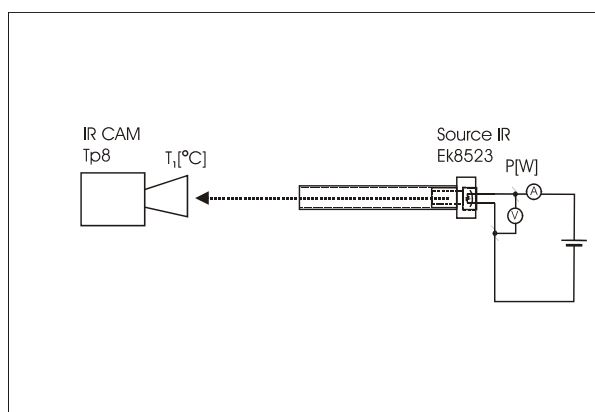


Fig. 11 Measuring workplace with thermal imager

#### Main technical specification of infra camera

| Imaging Performance  |   |
|----------------------|---|
| THERMAL              |   |
| Detector type:       | Uncooled FPA microbolometer (384× 288 pixels, 35μm) |
| Spectral Range:      | 8-14μm  |
| Thermal Sensitivity: | 0.08°C at 30°C (Frame averaging algorithm)          |

#### Main specification of IR source EK-8520

##### Key Features:

Kanthal Filament with Emissivity of 0.7

No Window

Internal Gold Plated Parabolic Reflector

Industry Standard TO-8 Package

##### Electrical Specifications:

Peak Voltage = 3.0 V DC

Peak Current = 1.48 A

Peak Power = 4.4 W

|                                   |   |
|-----------------------------------|---|
| Field of View/ Focus:             | 22°× 16°/ 35mm  |
| Focus:                            | Automatic or motorized  |
| Electronic Zoom:                  | ×1 to ×10 continuous zoom   |
| VISUAL                            |   |
| Built-in Digital Video:           | CMOS Sensor, 1280× 1024 pixels, 2 <sup>16</sup> colors  |
| Image Presentation                |   |
| External Display:                 | 3.5" high resolution color VGA LCD, 640× 480 pixels   |
| Viewfinder:                       | 0.6" built-in high resolution color OLED, 640× 480 pixels   |
| Video Output:                     | VGA/PAL/ NTSC switchblade   |
| Man-Machine Communication         |   |
| Touch Screen:                     | Present and receive operator's commands given by touch  |
| Auto Speech Recognition System:   | Automatically recognize and react to operators' voice commands                                    |
| Remote Control Handle (optional): | Respond as per operators' operation   |
| Joystick & Buttons:               | Respond as per operators' operation   |
| Menu:                             | Microsoft® Windows style  |
| Measurement                       |   |
| Temperature Range:                | Filter 1: -20 °C- +250°C;<br>Filter 2: 200°C- +800°C (up to +2000°C optional)                     |
| Accuracy:                         | Filter 1: ±1°C or ±1% of reading;<br>Filter 2: ±2°C or ±2% of reading                             |
| Measurement Modes:                | Auto hot spot & auto alarm in live/ zoomed image & video; 8 movable spots, 8 movable & changeable |

|  |  |
|--|--|
|  | areas displaying either max, min, or average, vertical & horizontal line profile, histogram & isotherm in live/zoomed/frozen/saved image & video |
| Emissivity Correction:                       | Variable from 0.01 to 1.00 (in 0.01 increment)   |
| Measurement Features:                        | Automatic correction based on distance, relative humidity, atmospheric transmission and external optics  |
| Optics Transmission Correction:              | Auto, based on signals from sensors  |
| Image Storage                                |  |
| Type:  | Removable 2GB SD card or built-in flash memory   |
| File Format:                                 | JPEG (An individual file consists of infrared image, visual image, voice annotation and text annotation if any)                                  |
| Voice Annotation:                            | Up to 30 seconds per file (More than 30 seconds optional)<br>Bluetooth wireless headset  |
| Text Annotation:                             | Selected from preset texts   |
| Live Video Recording & Measurement & Storage |  |
| Recording:                                   | Thermal video recording to PC via USB2.0   |
| Measurement:                                 | The same as image  |
| Storage:                                     | In PC, capacity dependent on PC hard disk capacity   |
| Optional Lenses                              |  |
| Field of View/ Focus:                        | 7.7°× 5.8°/ 100mm<br>45.6°× 35°/ 16mm  |
| Laser Locator                                |  |
| Classification Type:                         | Class 2 semiconductor laser  |

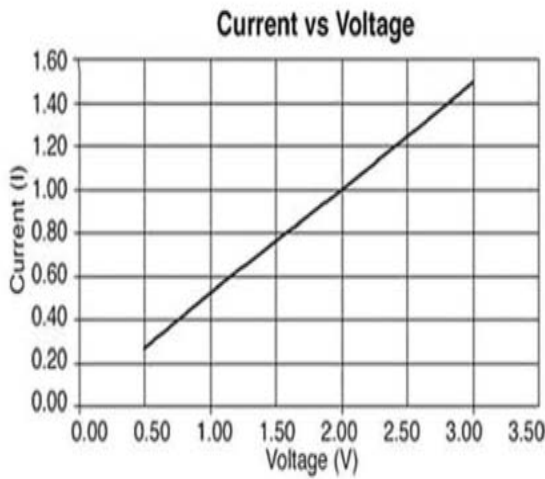


Fig. 12 Current vs Voltage of EK-8520

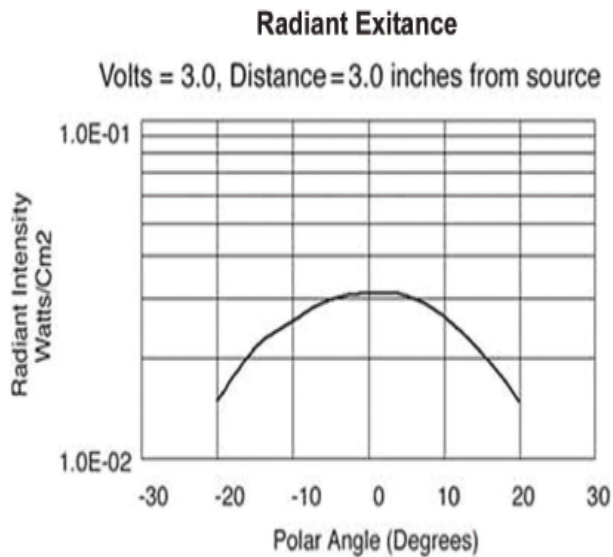


Fig. 13 Radiant Exitance

III. PROBLEM SOLUTIONS

Measured values for filter 1 for measuring temperatures in the range - 20 to + 250 ° C, emissivity  $\epsilon_1 = 0.7$  for kanthal wire are placed in table 1. The values was measured for IR emitters without windows and surface of the inner tube flat  $S_1 = \pi \cdot D_2 / 4 = 2.54 \text{ cm}^2$ .

The values for filter 2 with range IR camera for the + 200 to + 800 ° are in table 2. The values of  $Q_B$  and  $\lambda_{\text{max}}$  are then calculated according to formulas (3) and (5).

Table 1 Measured values temperature for filter 1

| Filter | Voltage | Current | Power  | Temp   | EmitEn    | $\lambda_{\text{max}}$ |
|--------|---------|---------|--------|--------|-----------|------------------------|
| 1, 2   | U[mV]   | I[mA]   | P[W]   | T1[°C] | $Q_B$ [W] | [ $\mu\text{m}$ ]      |
| 1      | 321,2   | 140,0   | 0,0450 | 24,60  | 0,0794    | 9,733                  |
| 1      | 404,0   | 170,0   | 0,0687 | 25,60  | 0,0805    | 9,700                  |
| 1      | 554,0   | 240,0   | 0,1330 | 31,30  | 0,0868    | 9,518                  |
| 1      | 748,0   | 320,0   | 0,2394 | 35,60  | 0,0918    | 9,386                  |
| 1      | 986,0   | 430,0   | 0,4240 | 45,80  | 0,1045    | 9,086                  |
| 1      | 1 149,0 | 500,0   | 0,5745 | 58,10  | 0,1216    | 8,748                  |
| 1      | 1 580,0 | 690,0   | 1,0902 | 75,60  | 0,1494    | 8,309                  |
| 1      | 1 831,0 | 790,0   | 1,4465 | 88,90  | 0,1736    | 8,004                  |
| 1      | 2 108,0 | 900,0   | 1,8972 | 110,30 | 0,2184    | 7,558                  |
| 1      | 2 949,0 | 1 260,0 | 3,7157 | 140,60 | 0,2960    | 7,004                  |

Table 2 Measured values temperature for filter 2

| Filter | Voltage | Current | Power  | Temp   | EmitEn    | $\lambda_{\text{max}}$ |
|--------|---------|---------|--------|--------|-----------|------------------------|
| 1, 2   | U[mV]   | I[mA]   | P[W]   | T1[°C] | $Q_B$ [W] | [ $\mu\text{m}$ ]      |
| 2      | 1 412,0 | 610,0   | 0,8613 | 281,80 | 0,9580    | 5,222                  |
| 2      | 1 674,0 | 730,0   | 1,2220 | 315,50 | 1,2128    | 4,923                  |
| 2      | 1 879,0 | 810,0   | 1,5220 | 355,40 | 1,5766    | 4,611                  |
| 2      | 2 146,0 | 930,0   | 1,9958 | 404,70 | 2,1326    | 4,275                  |
| 2      | 2 361,0 | 1 020,0 | 2,4082 | 456,60 | 2,8646    | 3,971                  |
| 2      | 2 473,0 | 1 070,0 | 2,6461 | 482,30 | 3,2899    | 3,836                  |
| 2      | 2 878,0 | 1 240,0 | 3,5687 | 528,60 | 4,1737    | 3,615                  |
| 2      | 3 253,0 | 1 390,0 | 4,5217 | 574,30 | 5,2098    | 3,420                  |
| 2      | 3 252,0 | 1 390,0 | 4,5203 | 578,10 | 5,3038    | 3,404                  |

The temperature dependence of the input power the source of infrared radiation EK 8320 is shown on Figure 3 and the dependence of the maximum wavelength of the source temperature on Figure 4.

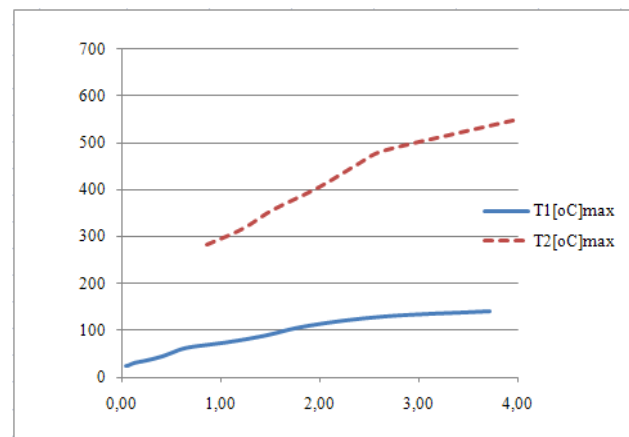


Fig. 14 Dependency  $T=f(P)$  for filter 1 a 2 of IR camera

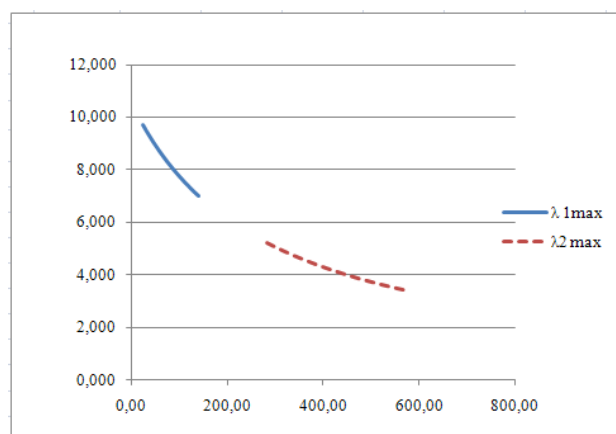


Fig. 15 Dependency  $\lambda_{\max}=f(T)$  for filter 1 a 2 of IR camera

#### IV. CONCLUSION

The graph in figure 14 shows that the quantity of heat energy that passes through the filter 1 is less than the amount of heat that passes through the filter 2, which is mainly due to characteristics of the filter of IR camera. Simultaneously  $Q_B$  energy radiated at low emitter power consumption is lower, that is caused that a certain quantity of heat energy of kanthal spiral at lower temperatures is taken into surround and absorbed into the brass holder.

The graph in figure 15 shows the dependence of  $\lambda_{\max} = f(T)$  and demonstrate, that at lower temperatures the maximum wavelength is shifted to the area about 9 mm, while at temperatures above 400 ° C is a maximum range below 4 mm. This is especially useful for security applications, where we need accurately define the characteristics of the IR source and then we can use it for testing of PIR detectors and directional characteristics statically and dynamically with possibility measuring of transition action.

#### V. LIST OF SYMBOLS

|             |                                       |                   |
|-------------|---------------------------------------|-------------------|
| $Q_0$       | transmission energy                   | $W/m^2$           |
| $S_1$       | square of body                        | $m^2$             |
| $T$         | absolute temperature of body          | K                 |
| $\delta_0$  | Stefan-Bolzman konstant               | $W m^{-2} K^{-4}$ |
| $L_\lambda$ | spectral radiation                    | $W m^2$           |
| $\lambda$   | wavelength                            | m                 |
| $\varphi_1$ | angle coefficient                     | -                 |
| $\tau_1$    | coeff. of penetration of Fresnel lens | -                 |
| $\tau_2$    | coeff. of penetration of filter       | -                 |
| $\rho_1$    | coeff. of reflection                  | -                 |
| $I$         | incident radiation                    | -                 |
| $E$         | emissivity                            | -                 |
| $R$         | reflection                            | -                 |
| $T$         | transmission                          | -                 |
| $A$         | absorption                            | -                 |

#### REFERENCES

- [1] D. Janáčová, "Modeling of Extraction Processes", Habilitation work, TBU Zlin, 2003. (in Czech)
- [2] K. Kolomazník, D. Janáčová, Z. Prokopová, "Modeling of Raw Hide Soaking", in *WSEAS Transactions on Information Science and Applications*, Hellenic Naval Academy, Ostrava Poruba, 2005.
- [3] K. Kolomazník, et al., *Modeling of dynamical systems*, Brno: VUT Brno, 1988. (in Czech)
- [4] J. Crank, *The Mathematics of Diffusion*, 2nd Ed. Clarendon Press, Oxford 1977.
- [5] D. Janáčová, et al., "Washing Processes Optimization", in *International Union of Leather Technologists and Chemists Societies*, London, 1997.
- [6] K. Kolomazník, T. Fürst, D. Janáčová, M. Uhlířová, V. Vašek, "Three Dimensional Transport Model Using in Soaking Process", in *WSEAS Transactions on Computer Research*, WSEAS World Science and Engineering Academy and Science, Queensland, 2007.
- [7] K. Kolomazník, D. Janáčová, V. Vašek, M. Uhlířová, "Control algorithms in a minimum of main processing costs for production amaranth hydrolyzates", in *WSEAS Transactions on Information Science and Applications*, WSEAS World Science and Engineering Academy and Science, Athens, 2006.
- [8] J. Dolinay, et al., "New Embedded Control System for Enzymatic Hydrolysis", in *Proceedings of the 8th WSEAS International Conference on Applied Informatics and Communications*, Rhodes, Greece, 2008, p. 174.
- [9] H. Charvátová, "Modeling of pelt chemical delimiting", Dissertation work. Tomas Bata University in Zlin, Zlin, 2007. (in Czech)
- [10] D. Janáčová, et al. "Modeling of non-stationary heat field in a plane plate for assymetric problem", in *14th WSEAS International Conference on Systems. Latest Trands on Systems. Volume II*, WSEAS Press (GR), Rhodes, 2010
- [11] O. Šuba, L. Sýkorová, Š. Šanda, M. Staněk, "Modelling of Thermal Stresses in Printed Circuit Boards", in *13th WSEAS International Conference on Automatic control, modelling & simulation (ACMOS'11)*, WSEAS Press, Lanzarote, Canary Islands 2011.
- [12] L. Vašek, V. Dolinay, „Simulation Model of Heat Distribution and Consumption in Municipal Heating Network”, in *14th WSEAS International Conference on Systems. Latest Trands on Systems. Volume II*, WSEAS Press (GR), Rhodes, 2010, p.439-442.

**Rudolf Drga** is an Associate Professor in the Department of Security Engineering, Faculty of Technology of Tomas Bata University in Zlín. His research activities include electronic security systems.

**Dagmar Janáčová** is an Associate Professor in the Department of Automation and Control Engineering, Faculty of Applied Informatics, of Tomas Bata University in Zlín. Her research activities include: modeling of treatment processes of natural polymers, transport processes, recycling of tannery wastes, and optimization and ecological approach of tannery processes. She has received the following honors: Diploma of England, XXIII IULTCS Congress, London, 11–14 September, 1997; Gold Medal - EUREKA EU Brussels 1997; Special Prize, Ministry of Agriculture, Belgium, 1997.

**Hana Charvátová** is a research worker at the Department of Automation and Control Engineering, Faculty of Applied Informatics, of Tomas Bata University in Zlín. Her research activities include recycling technology and modeling of natural and synthetic polymers processing.